Indoor air aerosol modeling and evaluation based on simulation chamber experiments

Corentin Berger, Maxence Mendez, Alice Micolier, Jean-Luc Ponche, Didier Hauglustaine, Nadège Blond

Modelling aerosols in indoor air: assessment with experiments in simulated atmosphere chambers

Corentin Berger[1,2,3], Nadège Blond[1], Maxence Mendez[3], Alice Micolier[3], Didier Hauglustaine[4], Jean-Luc Ponche[1]

[1]Université de Strasbourg, CNRS, Laboratoire Image Ville et Environnement (LIVE), UMR7362, Strasbourg, France
[2]French Environment and Energy Management Agency, Angers, France
[3]Octopus Lab, La Madeleine, France
[4]Laboratoire des Sciences du Climat et de l'Environnement, Gif-sur-Yvette, France

Correspondence to: Corentin Berger (corentin_berger@yahoo.fr)

Highlights.

- A new indoor air quality model describing both gas phase and phases.
- Assessments with experiments in simulated atmosphere chambers
- Analyses of diesel soot evolution and formation of secondary organic aerosol.

Abstract. High levels of PM in indoor environments is a great concern for human health. INCA-Indoor is an IAQ model which simulates more than 900 species in gas phase in indoor air. The present study details the aerosol module implemented in INCA-Indoor describing the processes at work in indoor air: aerosol formation by nucleation, growth of particles by coagulation or condensation, deposition and air exchanges between rooms, etc. To validate and assess the performance of the new modelling system, simulations were compared with measurements in an atmospheric simulation chamber. Two experiments from the EUROCHAMP-2020 database were selected with two different types of particles present in indoor air: growth of diesel soot in the AIDA chamber and SOA formation following ozonolysis of α-pinene in the EUPHORE chamber. The model simulations agree with measurements of the number of aerosols and their size distribution during the growth of diesel soot and their depositions. The mass concentration cannot be simulated due to the real diesel soot forms not spherical as in the model. The model reproduces the formation of aerosol from the ozonolysis of α-pinene in the gas phase, and allows to evaluate the competition between the nucleation of aerosol gas precursors and their condensation on existing particles and between coagulation and deposition afterwards. The work confirms experimental findings and associated assumptions regarding to the composition of the aerosols produced by this ozonolysis.

Keywords: Aerosol, Secondary Organic Aerosol, Coagulation, Condensation, Nucleation, Atmospheric simulation chamber

1. Introduction

People spend on average 80% of their time indoors where high levels of organics and particulate matter (PM) could be reached (*Morawska et al., 2017*). These particles come from indoor sources or outdoor-to-indoor exchanges. Direct indoor PM emissions may arise from occupants' activities (like tobacco smoking, cooking, rubbing of carpets or fabrics, etc), or from re-suspension after deposition (*Hussein et al., 2005, 2006*). Besides, terpenes, emitted during cleaning operations (*Singer et al., 2006*; *Nørgaard et al., 2014*) or cooking activities like orange peeling (*Vartiainen et al., 2006*), can react with oxidizing agents to form Secondary Organic Aerosols (SOA).

Primary and secondary PM induce many health effects, including pulmonary and cardiovascular diseases (*Shiraiwa et al., 2017*). Besides, they are vectors of organic pollutants, various allergens (*Blanchard et al., 2014*) or biological agents (*Fennelly et al., 2020*). To better evaluate health risks arising from PM in indoor environments, observation campaigns are necessary. The measurement campaign during the MERMAID project (*Schoemaecker et al., 2015*) made it possible to observe particles formation episodes in indoor air. Nevertheless, such observations are not sufficient to fully understand the processes impacting particles concentration as a function of the environmental conditions (e.g. location of the building, time of the day) or building design (ventilation system) and use (activities). Models are complementary tool that can help to detail the processes. Their developments need very precise measurement campaign in order to verify the modelling assumptions.

Most of the models simulating aerosols concentration indoors are aeraulic models in which only transport and deposition processes are included. For example, the Fate and Transport of Indoor Microbiological Aerosols (FaTIMA) tool is based on the NIST aeraulic models CONTAM to estimate the concentration of aerosols a person might encounter in a room (*Dols et al., 2020*). The Multichamber Indoor Air Quality model (MIAQ; *Nazaroff and Cass, 1986, 1989*) allows the simulations of the aerosol coagulation, deposition and exchanges. However, this model does not characterize the formation of SOA or the condensation of Semi-Volatile Organics (SVOCs) on aerosols. The Indoor Chemistry and Exposure Model (ICEM; *Sarwar et al., 2002, 2003*) has integrated particle chemistry for α-pinene as described by *Kamens et al.* (1999). This model accounts for the gas-particle transformation of semi-volatile products and particle growth by condensation of semi-volatile products onto existing particles. Indoor Detailed Chemical Model (IDCM; *Carslaw, 2007*; *Carslaw et al., 2012*; *Kruza et al., 2017*) calculates gas-to-particle partition for 41 species according to the absorptive partitioning theory of Pankow (1994). Calculations are made according to the total particle mass and the number distribution of particles is disregarded. In both IDCM and ICEM models, particles' growth is a function of condensation, and aerosols cannot coagulate together. The sectional aerosol model for submicron of *Asmi et al.* (2004) is currently one of the most complete models, considering nucleation, condensation, coagulation, deposition, effect of surface accumulation and exchanges with outdoor air. Simulated

values are in relatively good agreement with measurements realised in a large office building (*Koponen et al., 2001*) while the composition of particles is simplified and consists of water and some general condensable vapor.

The objective of this study is to present a new model designed to simulate both the gas and aerosol phases at the same time. The simulation of the aerosol phase covers all the processes impacting the particles from their formation to their growth and losses : coagulation, nucleation, condensation, indoor-outdoor exchange and deposition. This study also proposes a validation of the aerosol modelling based on very detailed experiments performed in atmosphere chambers in which particles are generated from the combustion of Diesel and ozonolysis of *α*-pinene. Diesel particle can be present indoor near heavy traffic roads, and *α*-pinene can be emitted by fragrances (ex: pine) in cleaning products. The two experiments were selected because performed in large room volumes too. The use of data from such experiments, performed under full controlled conditions, allows a full understanding and identification of the impact of modelled processed. It is a preliminary work performed with simple volume and surface, homogeneous and measured air conditions (temperature, humidity, etc.) before an application in real building, with complex forms and under uncontrolled conditions. The work is based on the INCA-Indoor model that was developed to simulate concentrations of various volatile organic compounds (VOCs) and oxidants in multi-rooms (*Mendez et al., 2015*). Thus, the SOA formation pathways and their compositions are identified through a precise characterization of the gas phase, and the aerosol phase both in number of aerosols, mass concentration, and composition.

The paper is organized as follows. The description of the aerosol module is exposed in *Section 2*. The methodology to evaluate the robustness of INCA-Indoor modelling is explained in *Section 3*. Simulation results are compared with experiments in simulation chambers in which particles are generated from the combustion of Diesel and ozonolysis of α-pinene, and discussed in *Section 4*.

2. INCA-Indoor model and its aerosol module

2.1. Gas phase INCA-Indoor model

INCA-Indoor is a box time-resolved numerical model developed from the INCA model (*Folberth et al., 2006*; *Hauglustaine et al., 2004*) in order to understand the physical and chemical processes leading to indoor air pollution and identifying the main contributions to pollutant concentrations. Most of the physics and chemistry of the INCA-Indoor gas-phase model is described in *Mendez et al.* (2015) for emissions, gas phase and heterogeneous chemistry, outdoor air exchange, deposition and sorption processes. Simplified chemical mechanisms from the SAPRC-07 database (*Carter, 2010*) are integrated into INCA-Indoor with 1400 reactions for 650 VOCs. The HONO formation mechanisms have been implemented in INCA-Indoor and detailed in *Mendez et al.* (2017b). The model was compared to IAQ reference models and used to understand the chemistry of oxidant species under different indoor

conditions (*Mendez et al., 2015, 2017a and 2017b*). A cleaning operation with *d*-limonene emission was already described using the model, but theses analyses only focused on the gas phase (*Mendez et al., 2015*). Since this reaction can lead to an aerosol formation, an aerosol module was integrated to complete the gas part relying on several species present in the chemical mechanism (see *Section 2.2*). The aerosol module can operate independently of the gas module, but the SOA formation needs the gas module to operate.

2.2. INCA-Indoor aerosol module

Aerosols are characterized by their size distributions and compositions. A sectional representation described by *Gelbard et al.* (1980) has been used: each section i is defined by a number N_i and a mass M_i concentration, a mean diameter d_i and a composition. A logarithmic distribution of sections by size is modelled on the *Scanning Mobility Particle Sizer* (SMPS). The logarithmic scale allows a good description of small particles without increasing the computation time and without losing accuracy to have a range amplitude of very large size. The sectional view allows to easily calculate the coagulation. For this study, the best trade-off between section resolution and computing time counts 8 channels per decade for a total of 32 size sections. The size range covered by INCA-Indoor is 21.6 nm to 216.5 µm for *Section 4.1* and 10.2 nm to 102.2 nm for *Section 4.2*, in order to cover the size ranges, determined by matching the SMPS size bins. As a first approximation as commonly done in air quality models, aerosols are considered as spherical in the model. The mass of particles can be computed from the number of particles, the average diameter of the aerosol section, considering that the aerosol is spherical. This approximation is usually used since no information on the aerosol forms is available. It cannot be used when studying diesel soot since we already know that diesel soot agglomerates are formed by chains of particles (see *Wentzel et al., 2003*).

The mean diameter, mass and number concentrations are calculated at each time step (here $t_{step} = 1min$) for 30 aerosol species with the nomenclature proposed by *Pun et al.* (2006) and considering surrogate SOA compounds and inorganic compounds. Except in very specific measurement studies, the composition of the particles is not studied and known. Since the composition of aerosols is unknown, generic species, representative of a family of real species, are used in INCA-Indoor : the surrogate BiA0D regroups carbonyl groups (i.e., aldehydes and ketones) and hydroxy groups (i.e., alcohols), the surrogate BiA1D regroups single carboxy groups. The surrogate BiA2D regroups two carboxy groups. In this work, we are only interested in the compounds produced by the ozonolysis of terpenes, BiA0D, BiA1D and BiA2D. Differentiating such species allows to indicate the composition of the different particle size classes considering their different chemical properties (vapor pressure, activity coefficient, enthalpy of vaporization, equilibrium constant, etc.). These chemical properties are given by the *Hydrophilic/Hydrophobic Organic* (H^2O) model that allows INCA-Indoor to compute the partitioning of species between the gas and aerosol phase. Aerosol concentration in each section is simulated

according to different processes such as the transport between rooms or indoor-outdoor, deposition on surfaces, growth either by coagulation between aerosols or by condensation of gases onto aerosol surface and the creation of particles by nucleation. The modeling of each process is detailed below. Fig.1 represents the different processes in the form of a diagram.

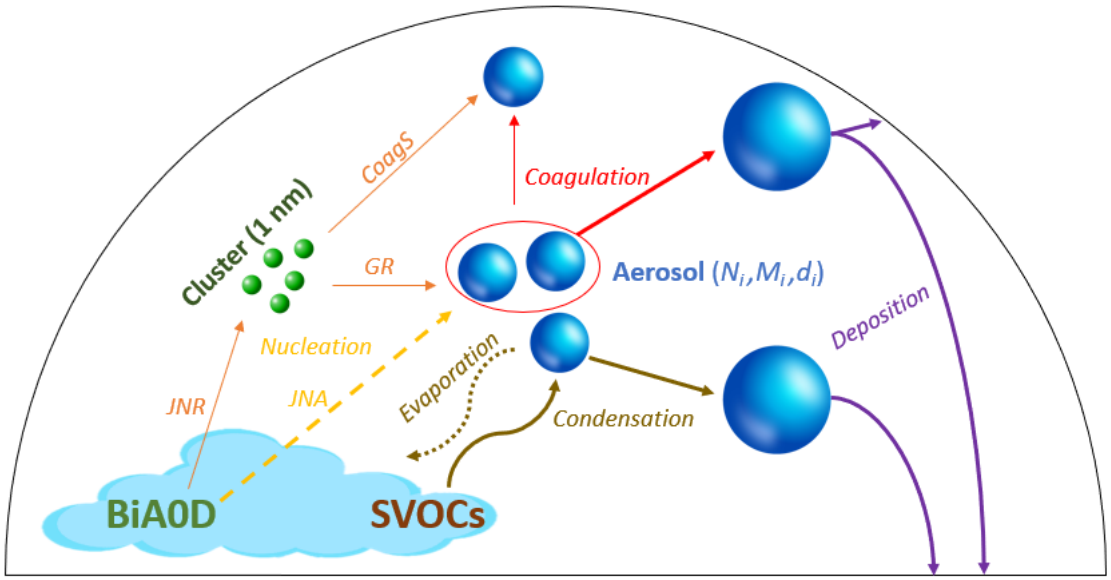

Fig. 1. Diagram of the processes modelled in the INCA-Indoor aerosol module (except aerosol transport) in an atmospheric simulation chamber.

2.2.1. Nucleation

In outdoor air quality model, BiA0D refers to biogenic species is often considered as a surrogate specie that can produce aerosols from nucleation. The formation of SOAs by BiA0D is considered as a reaction of second order governed by a nucleation rate. This nucleation rate was estimated based on the work of (*Kulmala et al., 2006*) on sulfuric acid particles : the nucleation is modelled considering two steps in order to simulate an aerosol formation directly in the first section of the model without detailing processes from the real nucleation of the particles (around 1 nm) and the growth to reach the range of our first modelled size section (*Kerminen and Kulmala,* 2002). A first cluster of particles with a diameter $d_n = 1nm$ is formed by the BiA0Ds with the "real" nucleation rate (JNR, $cm^3.s^{-1}$) (we called it "real" because the process is related to a real nucleation process but still it is an approximation since particles may have diverse diameters around 1 nm). Then, the particle growth to reach diameters in the range of our first modelled section. Two phenomena are in competition: (1) the cluster may grow by condensation of BiA0D until its diameter reaches the first section of the model (growth rate noted GR, $nm.s^{-1}$), (2) the cluster may also coagulate on large pre-existing particles (coagulation sink rate named $CoagS(d_n)$, s^{-1}).

In order to consider the competition between cluster coagulation with other particles and cluster growth by condensation, *Kerminen and Kulmala* (2002) and *Lehtinen et al.* (2007) proposed to express an "apparent" nucleation rate JNA ($cm^3.s^{-1}$) for aerosols of diameter d_1 as a function of JNR:

$$JNA = JNR\ exp\left(-\gamma d_n \frac{CoagS(d_n)}{GR}\right) \#(1)$$

where γ is a proportional factor (no unity). γ has been defined by *Lehtinen et al.* (2007). The coagulation sink $CoagS(d_n)$ is dependent on the particle size distribution and a coagulation rate (see *Section 2.2.2*) while the cluster growth rate by condensation GR is dependent on the concentration of BiA0D in the room. The mass of clusters formed was found to be negligible compared to the mass of the first-class particles and can be neglected.

As most of aerosol modelling studies, it was first assumed that a surrogate specie BiA0D could be considered as the nucleating species. The scheme then leads to a very high production of the small particles. Actually, few recent studies showed that aerosol nucleation is still a poorly described process and needs to be revised. Low-volatility carboxylic acids (C8–C10) were identified in the particulate phase (10 and 20 nm particles) as the major components of the SOA (*Yasmeen et al., 2010*; *Claeys et al., 2009*, *Winkler et al., 2012*), including terpenylic acid, cis-pinonic acid, and pinic acid (*Amin et al., 2013*). The ozonolysis process on alkenes can lead to the formation of Crigee intermediate and these bi-intermediate compound (very unstable) can be rearranged (intramolecular reaction) to give carboxylic acids. *Winkler et al.* (2012) estimated a saturation vapor pressure on the order of 10^{-11} atm or less for compounds responsible for growth of particles between 4-30 nm and 10^{-9} atm for compounds responsible for growth of particles larger than 30 nm, within the lower end of the previous measured saturation vapor pressures of C8–C18 monocarboxylic acids (10^{-11}~10^{-3} atm) (*Cappa et al., 2008*; *Tao and McMurry, 1989*). Several studies (*Liggio and Li, 2006a, 2006b*) also report an uptake of pinonaldehyde (usually included in the generic BiA0D specie) onto acidic aerosols higher than what could be predicted by assuming equilibrium between the gas and particle phases and no chemical reaction inside the particles. This phenomenon was attributed to oligomer and/or organosulfate formation. *Couvidat et al.* (2018) and *Tuovinen et al.* (2021) finally stated that BiA0D compounds are not able to condensate according to the kelvin effect but few of them, with low saturation vapor pressure, contribute to the growth of particle per condensation.

This present work proposes to keep the same aerosol formation mechanism as proposed in outdoor air quality model for BiA0D, but creating a new surrogate BiA0D' with a low saturation vapor pressure (see *Section 2.2.3*). The estimation of this new saturation vapor pressure is explained in *Section 4.2*.

2.2.2. Condensation

The *Hydrophilic/Hydrophobic Organic* (H^2O) model (*Couvidat et al., 2012*) is implemented to calculate the equilibrium between the gas phase and the aerosol phase. The condensation of twenty-nine species or groups of species on pre-existing particles is calculated by H^2O model. Two groups of species are distinguished by Couvidat's model: hydrophobic species which only condense on an organic phase and hydrophilic species which condense on an aqueous phase, and otherwise on an organic phase. The concentration of primary organic compounds depends on the amount of organic matter available for SVOCs to condense and the volatility of these compounds. The secondary organic compounds for hydrophilic acids consider the oligomerization and dissociation of organic acids at high pH thanks to large effective Henry's law constants. In the α-pinene ozonolysis experiment studied in this paper, the relative humidity was close to zero. The particle is dry and the saturated vapor pressure of each species gives the partition between the mass of gas and the mass aerosol of each species.

Finally, H^2O model gives the gas phase concentration and the aerosol phase concentration for the 29 species at thermodynamic equilibrium over one hour. Based on the work of *Li and Shiraiwa* (2019), the timescale of thermodynamic equilibrium is lower compared to the INCA-Indoor time step fixed in the two experiments ($t_{step} = 1min$) with a bulk diffusion ($2.57 \cdot 10^{-13}$ $m^2.s^{-1}$). The concentration of species that has condensed onto particles is distributed according to a ratio between the surface of particles in each section and the total surface of all particles.

More description of H^2O modelling can be found in *Couvidat et al.* (2012). Table 1 gives the saturation pressure used in INCA-Indoor for this paper.

Table 1. Properties of surrogate SOA species from *Couvidat et al.* (2012) and used in INCA-Indoor for this paper.

Surrogate	Molecular Structure	Molecular Weight ($g.mol^{-1}$)	Saturation vapor pressure (torr) at 298K
BiA0D	Pinonaldehyde	168	2.70×10^{-4}
BiA0D'	Pinonaldehyde	168	1.15×10^{-8}
BiA1D	Norpinic acid	170	2.17×10^{-7}
BiA2D	Pinic acid	186	1.43×10^{-7}

The saturation vapor pressure is fixed at a temperature of 298 K in the H^2O model. Uncertainties are noted in particular for the saturation vapor pressure of BiA0D and discussed in the *Section 4.2*.

2.2.3 Coagulation

As proposed by *Otto et al.* (1999), coagulation can be expressed as a collision between two particles due to the Brownian motion. The collision between two particles of same size (i.e. same section) or different

sections lead to one bigger particle that may keep in the same section of the initial particles, or be associated to another larger section with losses of particles in the initial ones. $Kcoag_{i,j}$ is the coagulation rate coefficient of the collision "reaction" between particles i and j. *Fuchs* (1934) calculates this coagulation coefficient based on two theories describing the transport of particles: 1- continuum diffusion when the distance between the two aerosols is greater than their respective mean free path λ_P, and 2- kinetic theory otherwise. The coagulation coefficient is adapted from the collision function for the quasi-continuum regime between two particles *i* and *j*:

$$Kcoag_{i,j} = 2\pi D_{i,j} d_{i,j} \beta(Kn_D) \#(2)$$

with the diffusion coefficient $D_{i,j} = D_i + D_j$ ($cm^2.s^{-1}$), the particle diameter $d_{i,j} = d_i + d_j$ (cm) and the Dahneke's function $\beta(Kn_D)$. This last function is defined according to the Knudsen number Kn_D, which is simpler to the one defined by Fuchs and Wright (1939) but still very close (the relative error is less than 1%):

$$\beta(Kn_D) = \frac{1 + Kn_D}{1 + 2Kn_D + 2Kn_D^2} \; with \; Kn_D = \frac{2\lambda_P}{d_{i,j}} \#(3)$$

2.2.4. Deposition

Two types of deposition are considered on inert surfaces: 1- gravitational sedimentation for horizontal surfaces and transport through the boundary layer due to Brownian diffusion and 2- turbulent diffusion for both vertical and horizontal surfaces. Particle flux density to surface due to deposition J through the boundary layer is defined as Eq. (4):

$$J = v_d N_\infty \#(4)$$

where v_d is the deposition velocity ($m.s^{-1}$), N_∞ is the particle concentration outside the concentration boundary layer.

J_i is described by a modified form of Fick's law by *Lai and Nazaroff* (2000). For the boundary layer adjacent to a vertical surface, J is given by Eq. (5a):

$$J = -(\varepsilon_p + D)\frac{\partial N}{\partial y} \#(5a)$$

where ε_p is the particle turbulent diffusivity ($m^2.s^{-1}$), D is the Brownian diffusivity of the particle ($m^2.s^{-1}$) and y is the distance to the surface (m).

For the boundary layer adjacent to a horizontal surface, the influence of gravity is considered with the particle settling velocity through the boundary layer v_s (m.s^{-1}). J is given by Eq. (5b):

$$J = -(\varepsilon_p + D)\frac{\partial N}{\partial y} \pm v_s N \#(5b)$$

Lai and Nazaroff (2000) assume that the deposition flux is constant in the concentration boundary layer. The particle concentration, distance from the surface, and deposition velocity are normalized respectively by the freestream particle concentration N_∞, friction velocity u^* and fluid kinematic viscosity ν_g to be dimensionless. Using the equations Eq. (4) – Eq. (5), the dimensionless deposition velocity can be expressed as follows Eq. (6):

$$v_d{}^+ = \begin{cases} \dfrac{v_s{}^+}{1 - \exp\left(-v_s{}^+ I\right)} \, upward\ surface, \\ \dfrac{v_s{}^+}{\exp\left(-v_s{}^+ I\right) - 1} \, downdard\ surface, \\ \dfrac{u^*}{I} \, vertical\ surface \end{cases} \#(6)$$

where $v_s{}^+ = v_s/u^*$, $v_d{}^+ = v_d/u^*$, $I = 1/v_d{}^+ = \int_{r^+}^{30} (\nu_g/(\varepsilon_p + D))dy^+$, $y^+ = yu^*/\nu_g$, $y^+ = y\,u^*/\nu_g$, $r^+ = (D/2)\,(u^*/\nu_g)$.

To solve these Euler equations, an analogy can be done with an electrical diagram (*Lai, 2005*) with resistors. The work of *Lai* (2005) is based on a system with four resistors allowing to calculate the deposition rate. The deposition rate is calculated for each size section.

2.2.5. Transport

INCA-Indoor is a multi-box time-resolved numerical model. INCA-Indoor considers a room as a box. Exchanges with outdoor through the building envelope, openings or the ventilation system, as well as exchanges between rooms through the walls or openings, vary in time as a function of the indoor-outdoor temperature difference and the wind speed for example. Airflows may be determined (not used in this study) thanks a tight-coupling with CONTAM (*Dols and Polidoro, 2020*), a multizone indoor air quality and ventilation analysis program developed by the *National Institute of Standards and Technology Technical* (NIST).

The number of particles in each section (N_i) is defined for a room x connected to outside and the other rooms y as Eq. (7):

$$\frac{\partial N_{i,x}}{\partial t} = \frac{Q_{out\to x}}{V_x} N_{out}(t) - \frac{Q_{x\to out}}{V_x} N_{i,x}(t) + \frac{Q_{y\to x}}{V_x} N_{i,y}(t) - \frac{Q_{x\to y}}{V_x} N_{i,x}(t) + Prod(N_{i,x}) - Sink(N_{i,x}) \#(7)$$

where S (m^2) and V (m^3) are respectively the surface and the volume of the room, Q ($m.s^{-1}$) is the flow and *Prod(N_i) and Sink(Ni)* are respectively the production and sink contributions on the particle concentrations through complex interactions between nucleation (a production process), condensation & coagulation (mixed of production & sink processes), and deposition (sink process). One room is studied in this study.

3 Experimental design

To validate the model that has been developed, two experiments were reproduced with different types of aerosol (primary aerosol and SOA). Data of these experiments were extracted from the database of atmospheric simulation chamber studies supplied by EUROCHAMP-2020 (Integration of European Simulation Chambers for Investigating Atmospheric Processes – towards 2020 and beyond – https://data.eurochamp.org/). These data collected for comparison between model and measurement come from measurements realized in atmospheric simulation chamber by *Karlsruhe Institute of Technology* (KIT) and *Centro de Estudios Ambientales del Mediterraneo* (CEAM).

The first experiment is based on a characterisation campaign of soot aerosols in the AIDA (*Aerosols, Interactions and Dynamics in the Atmosphere*) chamber of KIT. This is a cylindrical aluminium vessel of 84.3 m^3 volume (*Bunz et al., 1996*; *Kamm et al., 1999*), described by *Saathoff et al.* (2003). Diesel soot aerosols were generated with a Volkswagen 4 cylinder turbo Diesel engine (TDI, type1Z). To avoid unrealistically high trace gas concentrations in the AIDA chamber the dilute aerosol was passed through three denuders in series (to remove water vapour, volatile organic compounds and most of the NOx) (*Saathoff et al., 2003*). The number concentration of particles larger than 7 nm was measured continuously with two condensation particle counters (CPC 3022, TSI) and the number size distribution was scanned by a scanning mobility particle sizer (DMA 3071 and CPC 3010, TSI). Samples for total carbon/elemental carbon analysis were collected, on preheated (250°C) quartz fibre filters (47 mm diameter, MK360, Munktell) followed by coulometric analysis (Coulomat 702, Stroehlein). This experiment was described in *Saathoff et al.* (2003) and *Wentzel et al.* (2003). *Wentzel et al.* (2003) noted that there are Polycyclic Aromatic Hydrocarbons (PAHs) in the particle composition, but they quantified by comparison of measurement and COSIMA model that the aerosol dynamics is dominated by a rapid coagulation leading to a clear decrease in particle number and a significant growth of the particles and the mass evolution reflects the impact of sediment deposition and particle diffusion towards the chamber walls. The experiment is used here to assess the coagulation and deposition process calculated by INCA-Indoor, without considering the condensation/evaporation process.

The second experiment selected was conducted at the EUPHORE (*European Photoreactor*) chamber of the CEAM building, which is a Fluorine-Ethene-Propene (FEP) half-sphere with a volume of 200 m^3 (*Becker et al., 1996*). The case study is the ozonolysis of α-pinene and the formation of SOA after this reaction. 190 ppb of ozone was generated and 125.8 mg of α-pinene was injected in EUPHORE. Rapid mixing of the gas is achieved by two fans with a nominal throughput of 8000 $m^3.h^{-1}$ housed in the chamber (*Siese* et al., *2001).* Ozone and α-pinene were monitored during the experiment respectively with ozone analyser (ML9810) and Fourier-transform infrared spectroscopy (FTIR Nicoletet Magna 550). Scanning mobility particle sizer (DMA 3081 and CPC 3775, TSI) measures particle size distribution and the number total concentration of particles. Mass concentration is not directly measured by the SMPS. The mass concentration is derived from a calculation based on spherical particles with a given density (see Table 2) and the size distribution. A tapered element oscillating microbalance (TEOM) system is used to measure particle mass concentrations with an aerosol sampling temperature 50°C. The use of a TEOM system may lead to underestimation of the aerosol mass as discussed in *Sect.4.2* (*Tortajada-Genaro and Borrás, 2011*). This experiment allows the evaluation of the condensation process, acting with the coagulation.

In both experiments, a dilution factor is obtained by monitoring SF_6 concentration (99.9%, Messer Griesheim) as an inert tracer : this dilution is considered in INCA-Indoor as the air exchange between the chamber and the outside (Table 2). The dilution is related to pure air (without particles and chemical reactants) entering the chamber and compensating for the pumping of the measuring instruments (to maintain a uniform pressure). The experiments were performed in the dark and without the presence of other reactive compounds (like NO_X).

Table 2. Parameters used by INCA-Indoor to simulate experiments: diesel soot in the AIDA chamber (first row) and ozonolysis of α-pinene in the EUPHORE chamber (second row).

Aerosol species	Chamber	Volume (m^3)	Total surface (m^2)	Aerosol density ($g.m^{-3}$)	Dilution factor ($m^3.h^{-1}$)	T° (°C)	RH (%)
Diesel soot	AIDA	84.3	94.3	1.7	0.4418	24	33-43
SOA aerosols	EUPHORE	200	200	1.25	19.71	9-23	≈ 0

AIDA chamber and the EUPHORE chamber were represented in the model as vertical surfaces and horizontal surfaces. In INCA-Indoor, Diesel soot aerosols are generated in the AIDA chamber with a number size distribution identical to the first initial measures of SMPS. Temperature, pressure and relative humidity were monitored in the chamber for both experiments and were used as inputs into INCA-Indoor.

4. Results and discussion

4.1. Modelling diesel soot evolution in the AIDA chamber

Fig. 2 shows the growth of particles in the AIDA chamber as simulated by INCA-Indoor (dotted curves) and measured by the SMPS (plain curves) during the forty three hours following the introduction of diesel soot aerosols. Since the resolution for the granulometric sections is different between the model and the SMPS, the number of particles for each section have been normalized by the diameter for better comparison. At the beginning of the experiment (blue curve), the average diameter is 230 nm while after 40 hours (brown curve), the average diameter reaches 360 nm. Along with this growth, the total number of particles in the chamber decreases (Fig. 3). Indeed, in the absence of any condensable gas, the only way of growth is coagulation : coagulation lowers the number of particles without a reduction of the total mass. The work on coagulation proposed by *Otto et al.* (1999) is sufficient to describe the growth of Diesel soot. The rapid growth and decrease in particle number by coagulation calculated by INCA-Indoor are in good agreement with the results of *Wentzel et al.* (2003). The gas aspect, especially the condensation and evaporation processes are not integrated here and the model represents a simplistic, but effective view on particle growth and losses.

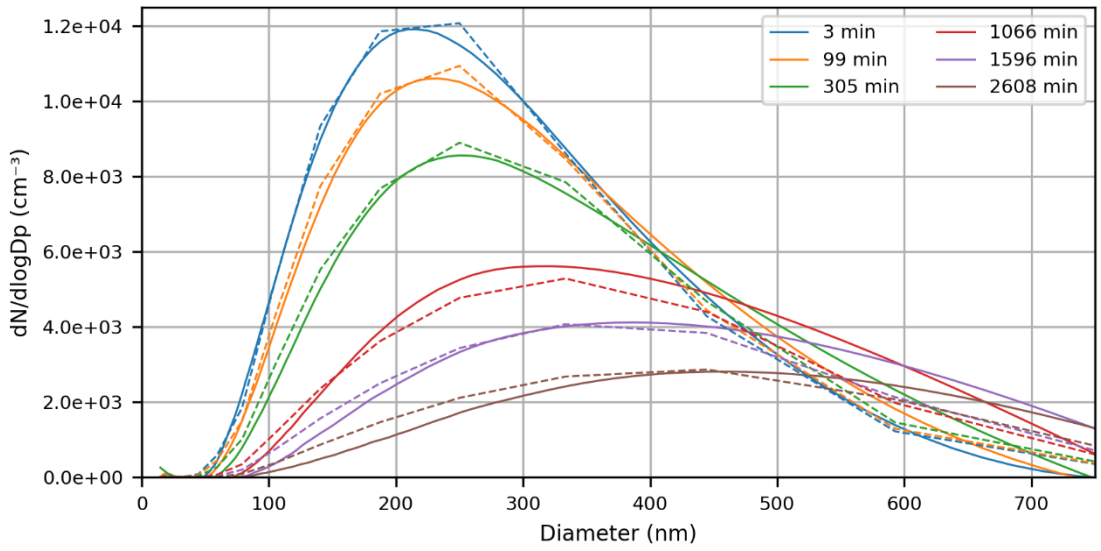

Fig. 2. Number size distribution of particles estimated from the SMPS measurements (plain curves) and simulated by INCA-Indoor (dotted curves) in the AIDA chamber.

The progressive decrease of the number of particles is linked to the deposition: in this experiment, this deposition represents 47 % of the particle mass loss. With the little air exchange in the chamber (≈ 0.5 $m^3.h^{-1}$), the phenomenon of deposition is here mainly governed by gravity.

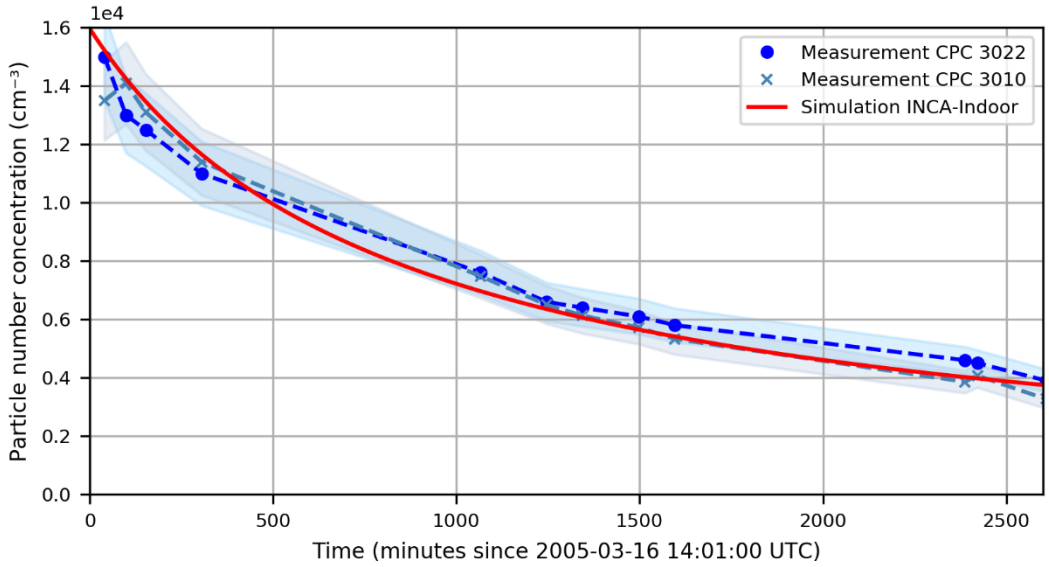

Fig. 3. Measured with CPC 3022 and CPC 3010 (blue dotted curve) and simulated by INCA-Indoor (red plain curve) particle number concentration in the AIDA chamber with measurement uncertainty band (blue area).

Different statistical tools such the *Normalized Mean Bias* (NMB), the *Normalized Mean Standard Deviation* (NMSD), Pearson's coefficient (ρ), Root Mean Square Error (RMSE) and *Model Quality Objective* (MQO) were calculated by comparison with the measurements of CPC 3022 and SMPS (DMA 3071 and CPC 3010) (Table 2) to assess the performance of the model. The MQO defined by *Thunis et al.* (2012) and based on the *Root Mean Square Error* (RMSE) and on the measurement uncertainty is less than 0.5 for the set of data issued from two measurement instruments. This means that the RMSE between the observed value and the simulated value is less important than the uncertainty on the measurement ($U = 10\ \%$). The model simulations are therefore in the uncertainty interval on the observation and the total number of particles simulated thus fits the measurements (Fig. 3), showing that the model faithfully transcribes the coagulation and deposit for Diesel soot particles.

Table 3. Statistical comparisons of total number concentrations modeled and observed during the growth of Diesel soot in the AIDA chamber.

Comparative measuring instrument	Normalized Mean Bias (NMB) (%)	Normalized Mean Standard Deviation (NMSD)	Pearson's coefficient (-1 < ρ < 1)	Root Mean Square Error (RMSE) (part./cm^3)	Model Quality Objective (MQO)
CPC 3022	- 0.28	0.10	0.996	$2.14 \cdot 10^3$	0.31

CPC 3010	4.28	0.12	0.990	$3.02 \cdot 10^3$	0.45

Mass concentration (total carbon) measured by particle collection on preheated quartz fibre filters followed by coulometric analysis cannot be since particles are considered to be totally spherical in INCA-Indoor. *Wentzel et al.* (2003) during the experiment show particles coagulated together forming characteristic chains with an average primary particle diameter of 27 ± 3 nm with a bulk material density of 1.7 $g.m^{-3}$ (*Wentzel et al., 2003*). Considering diesel soot as spherical particles lead to an overestimation of two observations of the mass concentrations : 266 (20 % at 70 min) and 209 $\mu g.m^{-3}$ (22 % at the end of the experiment). The simplistic view of INCA-Indoor provides a powerful tool for quantifying the distribution of aerosols in indoor air, but the assumption of aerosol sphericity is a limitation in the present version of INCA-Indoor to simulate any type of aerosols.

4.2. SOA in the EUPHORE chamber

To describe SOA formation in the EUPHORE chamber, the kinetics of the gas phase reaction must be well described. The mixing ratio of ozone and α-pinene are reproduced fairly faithfully compared to the measurements (Fig. 4). An overestimation of the ozone concentration has already been observed in other experiments (photo-oxidation of alkene) reproduced with the mechanism (MCMv3) in the EUPHORE Chamber (*Bloss et al., 2005*). Ozone loss is due to the reaction with α-pinene up to 94% at the start of the ozonolysis, and when α-pinene has been entirely consumed ozone loss is due to deposition. For α-pinene, the deposition and dilution are negligible compared to its consumption by its ozonolysis.

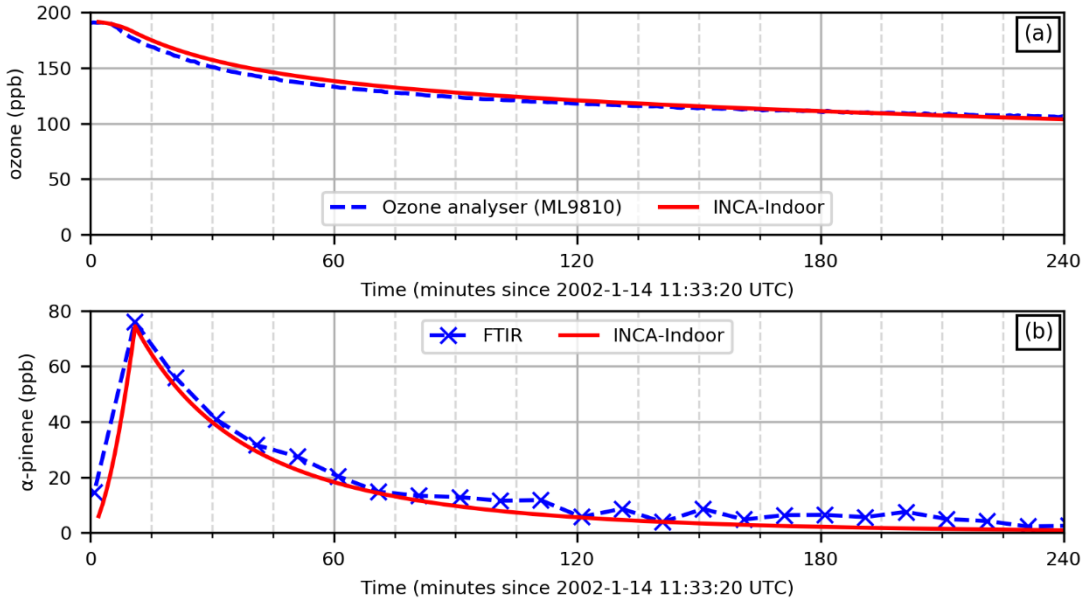

Fig. 4. Observed (blue dotted curves) and simulated (red plain curves) concentration of ozone (a) and α-pinene (b) in the EUPHORE chamber.

This reaction will produce several groups of species according to the chemical mechanisms SAPRC-07 database implemented in INCA-Indoor: BiA0D' (with the molecular structure of pinonaldehyde but with a lower vapor pressure), BiA1D (with the molecular structure of norpinic acid) and BiA2D (with the molecular structure of pinic acid). BiA0D' produced by the reaction will form the first small particles that are growing quickly (particles double their average diameter in about one hour after injection).

A competition sets in between nucleation and condensation. A saturated vapor pressure of BiA0D was initially set in the H^2O model to $Pvap_{sat}= 2.7 \cdot 10^{-4}$ Torr as proposed by *Coudivat et al.* (2012) for BiA0D (Table 1). But with such saturated vapor pressure value of BiA0D, BiA0D lead to the formation of a too large number of too small particles ($\approx 6 \cdot 10^6$ part./cm^3) compared with experiment. The saturated vapor pressure of BiA0D was reduced to $Pvap_{sat}= 1.15 \cdot 10^{-8}$ Torr to foster the condensation of BiA0D and in this way limit nucleation. Several works have shown that the saturated vapor pressure of pinonaldehyde is high compared to the equilibrium between the aerosol phase measured and the gas phase measured (*Tillmann et al., 2010*). This saturation vapor pressure difference can be explained by a heterogeneous reaction as the condensed phase oxidation of pinonaldehyde to pinonic acid (*Jenkin, 2004*). *Jenkin* (2004) had to artificially reduce the volatility of the products by a factor of 100 to explain the growth of SOA formed as a result of ozonolysis of α-pinene. This decrease in saturation vapor pressure is also discussed in *Sect.2.2.a*.

Fig. 5 represents the evolution of the particle size distribution as a function of the time. The average of all aerosols present in the chamber was represented by a black line on this figure. INCA-Indoor calculates 32 particle size classes (Res = 8) while the SMPS has a finer resolution (Res = 64). However, we observe the same quick particle growth: 40 nm to 100 nm in one hour for observation and 30 nm to 120 nm for simulation. The particle size distribution follows a '*banana plot*' characteristic of ozonolysis with two phases combined: SOA formation (see the colour tends towards the red in Fig. 5) and SOA growth (see the black curve of the mean diameter increases in Fig. 5). The particle growth calculated by the INCA-Indoor model is faster than the measurement. After 4 h, the mean diameter of the aerosols is greater than 150 nm for the model whereas it is never exceeded for observation. The SOA formation has been reproduced with INCA-Indoor and the works of *Kerminen and Kulmala* (2002) and *Lehtinen et al.* (2007) on the nucleation of sulfuric acid can be used with confidence to represent SOA formation.

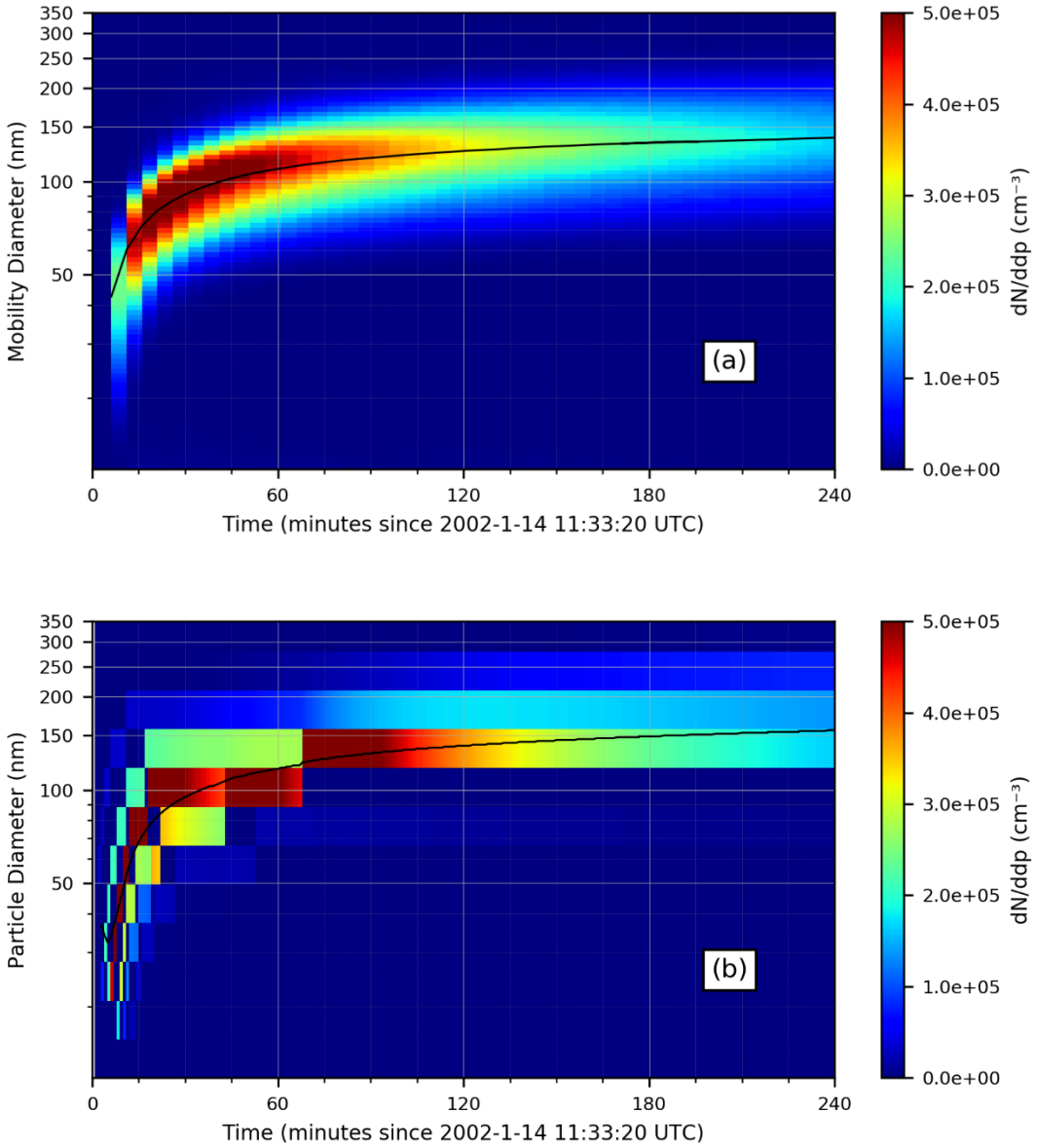

Fig. 5. Number size distribution and mean diameters for all particles (black line) in the EUPHORE chamber measured by SMPS (a) and simulated by INCA-Indoor (b).

The concentration in number and in mass for particles in EUPHORE increase from the start of the ozonolysis and a maximum of concentration number is reached after the injection of α-pinene (Fig. 6a). The formed clusters grow to the first class described by the model. The coagulation of clusters by larger particles is at its minimum at the beginning of the experiment. There is no loss of clusters and the nucleation is not limited. Then, the particle number concentration decreases while the mass concentration continues to increase (Fig. 6b). Indeed, from that moment on, there is no more nucleation (JNA close to zero) because the coagulation loss of clusters becomes predominant in relation to their growth. BiA0D' favors condensation on existing particles in relation to nucleation. In addition to condensation, the particles will coagulate and increase in size at the expense of the number of particles.

Work of *Otto et al.* (1999) on coagulation is based on primary aerosols with different physico-chemical properties and different processes. INCA-Indoor describes a strong coagulation which decreases the number concentration more than the measurement.

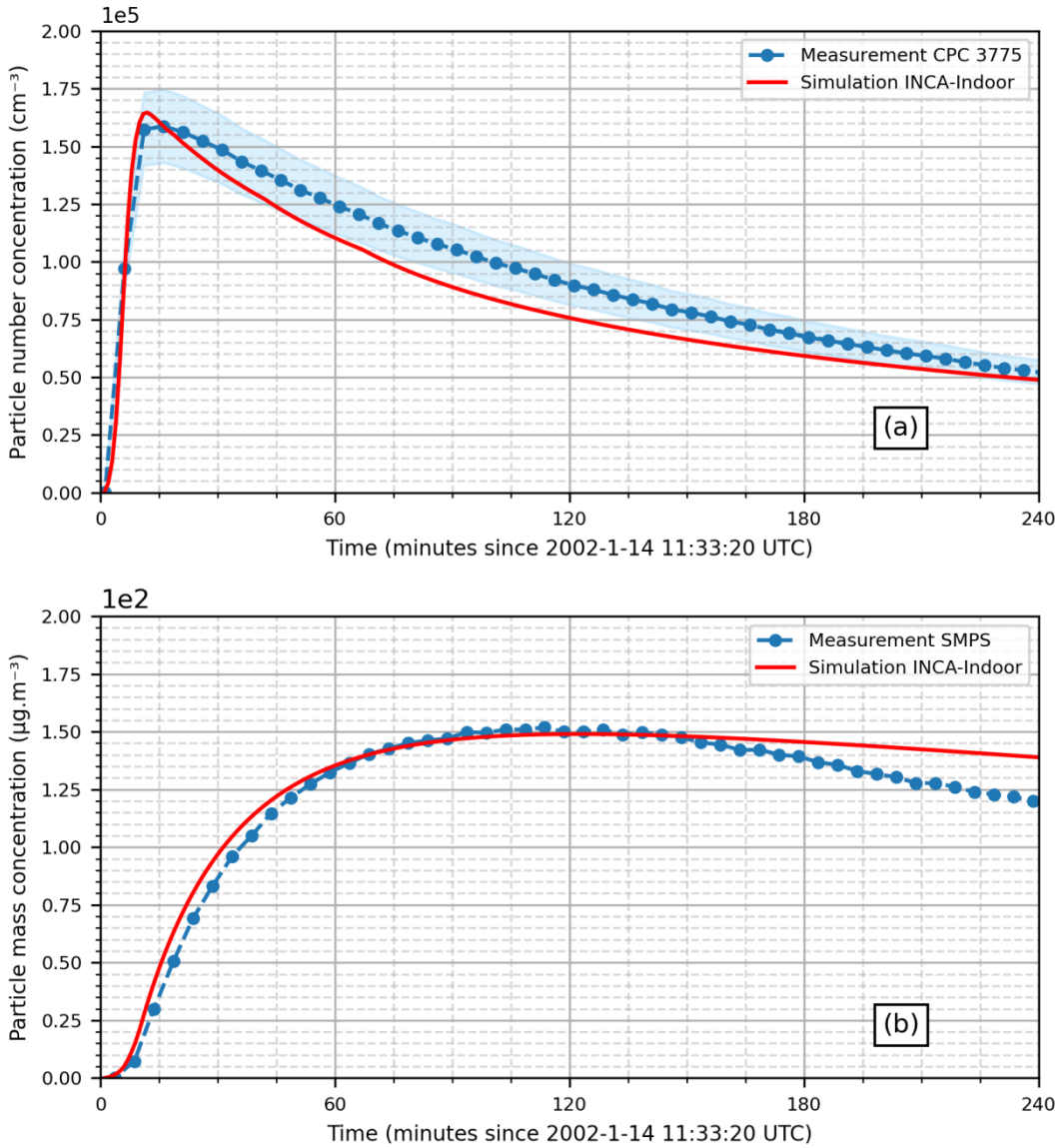

Fig. 6. Modeled and simulated particle number concentration (a) and mass concentration (b) in the EUPHORE chamber.

The same statistical tools as in Table 3 were calculated by comparisons between measurements and simulations of the total particle number concentration (Table 4). It shows a relatively small error which shows the good performance of the model in describing the concentration in numbers. The calculation of the MQO indicator between the total number concentrations measured and modelled was done on two different times: over the first hour (where there is formation of aerosols and a rapid growth linked to the condensation and coagulation), and over four hours. The MQO over the first hour is less than 0.5. The model succeeds in transcribing the nucleation of SOA and their growth by condensation mainly. After this formation phase, the two dominant processes are deposition and coagulation. A too high

coagulation probably explains that the MQO is higher over 4 h. With MQO > 0.5, RMSE is on average larger than the uncertainty interval on the observation, but the precise characterization of the concentration of particles is very variable according to the measuring instruments used.

Table 4. Statistical comparisons of total number concentrations modeled and observed during the α-pinene ozonolysis in the AIDA chamber.

Comparative measuring instrument	Normalized Mean Bias (NMB) (%)	Normalized Mean Standard Deviation (NMSD)	Pearson's coefficient ($-1 < \rho < 1$)	Root Mean Square Error (RMSE) (part./cm^3)	Model Quality Objective (MQO)	
					1 h	4 h
CPC 3775	-6.88%	- 0.016	0.98	$7.87 \cdot 10^4$	0.38	0.62

The contribution of the processes in mass and number concentration and in size is calculated by INCA-Indoor which allows to understand the aerosol formation and their growth (Table 5). Looking at the concentration in number, the source of aerosols is due to the nucleation and the main way of losses are the coagulation in favor of an increase in size. The major contribution in mass concentration production is the condensation of gases on aerosols formed by nucleation : The growth in size is linked to 25% by coagulation and 75% by condensation. The mass concentration decreases led by dilution, with a contribution of 10 to 40 % of the total losses during the experience, and deposition with a contribution of 60 to 90 %. The deposition velocity of the aerosols on the horizontal surface led by the gravitational settling is in the same range as their deposition velocity on the vertical surface led by the Brownian and turbulent diffusion, with a mean aerosol deposition velocity $v_d = 1.7 \cdot 10^{-5}$ cm.s^{-1} for each surface. The turbulent diffusion is accelerated by the fans which allow a rapid mixing of reagents and increase the impact of particles on the walls. The gap of the mass concentration between SMPS and INCA-Indoor after 140 min (Fig. 6b) could be explained by an underestimated deposition in our model. The EUPHORE chamber is actually a hemisphere while, in order to facilitate calculations, a vertical surface and a horizontal surface have been described in INCA-Indoor and could thus lead to an error in the estimation of the deposition rate.

Table 5. Contribution of physico-chemical processes on aerosol mass and number concentration calculated by INCA-Indoor during the experiment in EUPHORE chamber.

Physico-chemical process	*Nucleation*	*Coagulation*	*Condensation*	*Deposition*	*Dilution*
Contribution on number concentration (#/cm^3)	$+1.9 \cdot 10^5$	$-1.2 \cdot 10^5$	-	$-0.3 \cdot 10^5$	$-0.1 \cdot 10^5$

Contribution on mass concentration ($\mu g.m^{-3}$)	+0.2	-	+174	-41	-22

The model can provide an estimation of the aerosol composition that cannot be controlled by any observations : modeled aerosols are composed of 75 % of BiA0D' brought by nucleation and by condensation, and 25 % of BiA2D brought by condensation. This is a simplified view of the model with three groups of species. There are undoubtedly several species present in the particle and not modeled.

Different SVOCs condensation configurations were simulated allowing (1) only BiA0D' condensation, (2) only BiA0D' and BiA1D condensation, BiA0D' and BiA2D condensation, (3) condensation of all VOCs and with condensation on surface. The results in mass concentration with condensation of BiA0D' and BiA2D and without condensation on the surfaces are the closest to the measurements and it is these results that have been presented in this article. Varying such condensation options, the composition of SOA appears to vary considerably depending on the experiments and the experimental conditions. A future perspective is to compare the modeled compositions with measurements issued from a dedicated experiment.

5 Conclusion

The INCA-Indoor model was developed to characterize the gas phase in indoor air. A development of an aerosol module has been proposed in this article with different processes described: the nucleation of SOAs, aerosols growth by condensation or by coagulation and their losses by deposition or by exchange. The advantage of the INCA-Indoor model is to combine a gas phase well characterized and a coverage of the many processes impacting aerosols in indoor air. The validation is done by an comparison between simulations and measurements on controlled experiments that are typical from indoor air: the growth of characteristic particles from the outside (diesel soot) and formation of SOA.

The study allows to quantify the contribution of each process on size distribution and on total concentration in number and in mass. Coagulation is the only growth path in the AIDA chamber, the same situation is found for SOA in the EUPHORE chamber when nucleation and condensation are completed. There is a large loss in numbers through coagulation, but the mass concentration is preserved. The mass losses in both experiments are deposition and air exchange. Deposition in the AIDA chamber is largely governed by gravity, whereas in the EUPHORE chamber deposition by Brownian motion and turbulent diffusion dominates, especially with fans. These experiments make it possible to develop strategies for limiting the concentration of particles in indoor air according to their size by playing on the air renewal or the deposition

The model showed good performance in simulating the growth of aerosols, especially diesel soot. Particle number concentration calculated by the model in both chambers is in the measurement uncertainty band (MQO < 1). Particle size distribution during α-pinene ozonolysis or diesel soot growth is well described. This is major step forward in aerosol simulation because INCA-Indoor allows to evaluate simultaneously aerosols size, aerosol composition, number and mass concentration. The evaluation of the size of the particles can thus allow to identify the deposition areas in the respiratory tract after inhalation (*Lippmann and Albert, 1969*) and identify their capacity to be vectors of pollutants or biological agents (*Fennelly, 2020*). However, particle inhalation is probably a much more complex process to model because of the high relative humidity. Some aerosols (<5 µm) contain SARS-CoV-2 (*Van Doremalen et al., 2020*). The INCA-Indoor aerosol module is currently used to determine the risk of spreading the virus within a building (*Micolier et al. 2020*).

INCA-Indoor is a now a model able to fully simulate air quality in buildings, and this way constitutes a decision-making tool to guide building design by identifying the processes and sources of pollutants. A perspective for the model is to assess the quality of the predictions for aerosols in real-world settings with indoor-outdoor transport and occupants' influence. It will necessary to implement particles resuspension since it has been identified as an important source of particles in indoor air (*Benabed and Limam, 2017*).

Data availability

The data used are issued from the database of atmospheric simulation chamber studies supplied by EUROCHAMP-2020 (Integration of European Simulation Chambers for Investigating Atmospheric Processes – towards 2020 and beyond, https://data.eurochamp.org/, last access: March 2021).

Acknowledgements

We thank ADEME, Octopus Lab, and the Fonds de dotation AIR for providing the financial supports. We acknowledge the Mediterranean Center for Environmental Studies Foundation (CEAM) and Karlsruher Institut für Technologie (KIT) for accessing their high quality data and their experience in the EUROCHAMP-2020 database.

References

Amin, H. S., Hatfield, M. L., & Huff Hartz, K. E. (2013). Characterization of secondary organic aerosol generated from ozonolysis of α-pinene mixtures. *Atmospheric Environment*, *67*, 323–330. https://doi.org/10.1016/j.atmosenv.2012.10.063

Asmi, A. J., Pirjola, L. H., & Kulmala, M. (2004). A sectional aerosol model for submicron particles in indoor air. *Scandinavian Journal of Work, Environment & Health*, *30 Suppl 2*, 63–72.

Becker, K. H., Hjorth, J., Le Bras, G., Millán, M. M., Platt, U., Toupance, G., & Wildt, J. (1996). *The European Photoreactor: Euphore.* Wuppertal: European Commission.

Benabed, A., & Limam, K. (2017). Resuspension of Indoor Particles Due to Human Foot Motion. *Energy Procedia*, *139*, 242–247. https://doi.org/10.1016/j.egypro.2017.11.203

Blanchard, O., Glorennec, P., Mercier, F., Bonvallot, N., Chevrier, C., Ramalho, O., Mandin, C., & Bot, B. L. (2014). Semivolatile Organic Compounds in Indoor Air and Settled Dust in 30 French Dwellings. *Environmental Science & Technology*, *48*(7), 3959–3969. https://doi.org/10.1021/es405269q

Bloss, C., Wagner, V., Bonzanini, A., Jenkin, M. E., Wirtz, K., Martin-Reviejo, M., & Pilling, M. J. (2005). Evaluation of detailed aromatic mechanisms (MCMv3 and MCMv3.1) against environmental chamber data. *Atmospheric Chemistry and Physics*, *5*(3), 623–639. https://doi.org/10.5194/acp-5-623-2005

Bunz, H., Möhler, O., Naumann, K.-H., Saathoff, H., Schöck, W., & Schurath, U. (1996). *The Novel Aerosol Chamber Facility AIDA: Status and First Results*. "Proceedings of the EU Air Pollution Symposium '96, Venice, Italy.

Cappa, C. D., Lovejoy, E. R., & Ravishankara, A. R. (2008). Evidence for liquid-like and nonideal behavior of a mixture of organic aerosol components. *Proceedings of the National Academy of Sciences*, *105*(48), 18687–18691. https://doi.org/10.1073/pnas.0802144105

Carslaw, N. (2007). A new detailed chemical model for indoor air pollution. *Atmospheric Environment*, *41*(6), 1164–1179. https://doi.org/10.1016/j.atmosenv.2006.09.038

Carslaw, N., Mota, T., Jenkin, M. E., Barley, M. H., & McFiggans, G. (2012). A Significant Role for Nitrate and Peroxide Groups on Indoor Secondary Organic Aerosol. *Environmental Science & Technology*, *46*(17), 9290–9298. https://doi.org/10.1021/es301350x

Carter, W. P. L. (2010). Development of the SAPRC-07 chemical mechanism. *Atmospheric Environment*, *44*(40), 5324–5335. https://doi.org/10.1016/j.atmosenv.2010.01.026

Claeys, M., Iinuma, Y., Szmigielski, R., Surratt, J. D., Blockhuys, F., Van Alsenoy, C., Böge, O., Sierau, B., Gómez-González, Y., Vermeylen, R., Van der Veken, P., Shahgholi, M., Chan, A. W. H., Herrmann, H., Seinfeld, J. H., & Maenhaut, W. (2009). Terpenylic Acid and Related Compounds from the Oxidation of α-Pinene: Implications for New Particle Formation and Growth above Forests. *Environmental Science & Technology*, *43*(18), 6976–6982. https://doi.org/10.1021/es9007596

Couvidat, F., Debry, É., Sartelet, K., & Seigneur, C. (2012). A hydrophilic/hydrophobic organic (H 2 O) aerosol model: Development, evaluation and sensitivity analysis: H 2 O---A MODEL TO PREDICT ORGANIC AEROSOL. *Journal of Geophysical Research: Atmospheres*, *117*(D10), n/a-n/a. https://doi.org/10.1029/2011JD017214

Couvidat, F., Vivanco, M. G., & Bessagnet, B. (2018). Simulating secondary organic aerosol from anthropogenic and biogenic precursors: Comparison to outdoor chamber experiments, effect of oligomerization on SOA formation and reactive uptake of aldehydes. *Atmospheric Chemistry and Physics*, *18*(21), 15743–15766. https://doi.org/10.5194/acp-18-15743-2018

Dols, W. S., & Polidoro, B. J. (2020). *CONTAM User Guide and Program Documentation Version 3.4*. National Institute of Standards and Technology. https://doi.org/10.6028/NIST.TN.1887r1

Fennelly, K. P. (2020). Particle sizes of infectious aerosols: Implications for infection control. *The Lancet Respiratory Medicine*, *8*(9), 914–924. https://doi.org/10.1016/S2213-2600(20)30323-4

Folberth, G. A., Hauglustaine, D. A., Lathière, J., & Brocheton, F. (2006). Interactive chemistry in the Laboratoire de Météorologie Dynamique general circulation model: Model description and impact analysis of biogenic hydrocarbons on tropospheric chemistry. *Atmospheric Chemistry and Physics*, *6*(8), 2273–2319. https://doi.org/10.5194/acp-6-2273-2006

Fuchs, N. (1934). Zur Theorie der Koagulation. *Zeitschrift Für Physikalische Chemie*, *171A*(1), Article 1. https://doi.org/10.1515/zpch-1934-17116

Fuchs, W. H. J., & Wright, E. M. (1939). THE 'EASIER' WARING PROBLEM. *The Quarterly Journal of Mathematics*, *os-10*(1), 190–209. https://doi.org/10.1093/qmath/os-10.1.190

Gelbard, F., Tambour, Y., & Seinfeld, J. H. (1980). Sectional representations for simulating aerosol dynamics. *Journal of Colloid and Interface Science*, *76*(2), 541–556. https://doi.org/10.1016/0021-9797(80)90394-X

Hauglustaine, D. A., Hourdin, F., Jourdain, L., Filiberti, M.-A., Walters, S., Lamarque, J.-F., & Holland, E. A. (2004). Interactive chemistry in the Laboratoire de Météorologie Dynamique general circulation model: Description and background tropospheric chemistry evaluation: INTERACTIVE CHEMISTRY IN LMDZ. *Journal of Geophysical Research: Atmospheres*, *109*(D4), n/a-n/a. https://doi.org/10.1029/2003JD003957

Hussein, T., Glytsos, T., Ondráček, J., Dohányosová, P., Ždímal, V., Hämeri, K., Lazaridis, M., Smolík, J., & Kulmala, M. (2006). Particle size characterization and emission rates during indoor activities in a house. *Atmospheric Environment*, *40*(23), 4285–4307. https://doi.org/10.1016/j.atmosenv.2006.03.053

Hussein, T., Korhonen, H., Herrmann, E., Hämeri, K., Lehtinen, K. E. J., & Kulmala, M. (2005). Emission Rates Due to Indoor Activities: Indoor Aerosol Model Development, Evaluation, and Applications. *Aerosol Science and Technology*, *39*(11), 1111–1127. https://doi.org/10.1080/02786820500421513

Jenkin, M. E. (2004). Modelling the formation and composition of secondary organic aerosol from α- and β-pinene ozonolysis using MCM v3. *Atmospheric Chemistry and Physics*, *4*(7), 1741–1757. https://doi.org/10.5194/acp-4-1741-2004

K. Koponen, I., Asmi, A., Keronen, P., Puhto, K., & Kulmala, M. (2001). Indoor air measurement campaign in Helsinki, Finland 1999 – the effect of outdoor air pollution on indoor air. *Atmospheric Environment*, *35*(8), 1465–1477. https://doi.org/10.1016/S1352-2310(00)00338-1

K. Lai, A. C., & Nazaroff, W. W. (2000). MODELING INDOOR PARTICLE DEPOSITION FROM TURBULENT FLOW ONTO SMOOTH SURFACES. *Journal of Aerosol Science*, *31*(4), 463–476. https://doi.org/10.1016/S0021-8502(99)00536-4

Kalberer, M., Sax, M., & Samburova, V. (2006). Molecular Size Evolution of Oligomers in Organic Aerosols Collected in Urban Atmospheres and Generated in a Smog Chamber. *Environmental Science & Technology*, *40*(19), 5917–5922. https://doi.org/10.1021/es0525760

Kamens, R., Jang, M., Chien, C.-J., & Leach, K. (1999). Aerosol Formation from the Reaction of α-Pinene and Ozone Using a Gas-Phase Kinetics-Aerosol Partitioning Model. *Environmental Science & Technology*, *33*(9), 1430–1438. https://doi.org/10.1021/es980725r

Kamm, S., Möhler, O., Naumann, K.-H., Saathoff, H., & Schurath, U. (1999). The heterogeneous reaction of ozone with soot aerosol. *Atmospheric Environment*, *33*(28), 4651–4661. https://doi.org/10.1016/S1352-2310(99)00235-6

Kerminen, V.-M., & Kulmala, M. (2002). Analytical formulae connecting the "real" and the "apparent" nucleation rate and the nuclei number concentration for atmospheric nucleation events. *Journal of Aerosol Science*, *33*(4), 609–622. https://doi.org/10.1016/S0021-8502(01)00194-X

Kruza, M., Lewis, A. C., Morrison, G. C., & Carslaw, N. (2017). Impact of surface ozone interactions on indoor air chemistry: A modeling study. *Indoor Air*, *27*(5), 1001–1011. https://doi.org/10.1111/ina.12381

Kulmala, M., Lehtinen, K. E. J., & Laaksonen, A. (2006). Cluster activation theory as an explanation of the linear dependence between formation rate of 3nm particles and sulphuric acid concentration. *Atmospheric Chemistry and Physics*, *6*(3), 787–793. https://doi.org/10.5194/acp-6-787-2006

Lai, A. C. K. (2005). Modeling indoor coarse particle deposition onto smooth and rough vertical surfaces. *Atmospheric Environment*, *39*(21), 3823–3830. https://doi.org/10.1016/j.atmosenv.2005.02.055

Lehtinen, K. E. J., Dal Maso, M., Kulmala, M., & Kerminen, V.-M. (2007). Estimating nucleation rates from apparent particle formation rates and vice versa: Revised formulation of the Kerminen–Kulmala equation. *Journal of Aerosol Science*, *38*(9), 988–994. https://doi.org/10.1016/j.jaerosci.2007.06.009

Li, Y., & Shiraiwa, M. (2019). Timescales of secondary organic aerosols to reach equilibrium at various temperatures and relative humidities. *Atmospheric Chemistry and Physics*, *19*(9), 5959–5971. https://doi.org/10.5194/acp-19-5959-2019

Liggio, J., & Li, S.-M. (2006a). Organosulfate formation during the uptake of pinonaldehyde on acidic sulfate aerosols. *Geophysical Research Letters*, *33*(13), L13808. https://doi.org/10.1029/2006GL026079

Liggio, J., & Li, S.-M. (2006b). Reactive uptake of pinonaldehyde on acidic aerosols. *Journal of Geophysical Research*, *111*(D24), D24303. https://doi.org/10.1029/2005JD006978

Lippmann, M., & Albert, R. E. (1969). The Effect of Particle Size on the Regional Deposition of Inhaled Aerosols in the Human Respiratory Tract. *American Industrial Hygiene Association Journal*, *30*(3), 257–275. https://doi.org/10.1080/00028896909343120

Mendez, M., Amedro, D., Blond, N., Hauglustaine, D. A., Blondeau, P., Afif, C., Fittschen, C., & Schoemaecker, C. (2017). Identification of the major HO_x radical pathways in an indoor air environment. *Indoor Air*, *27*(2), 434–442. https://doi.org/10.1111/ina.12316

Mendez, M., Blond, N., Amedro, D., Hauglustaine, D. A., Blondeau, P., Afif, C., Fittschen, C., & Schoemaecker, C. (2017). Assessment of indoor HONO formation mechanisms based on in situ measurements and modeling. *Indoor Air*, *27*(2), 443–451. https://doi.org/10.1111/ina.12320

Mendez, M., Blond, N., Blondeau, P., Schoemaecker, C., & Hauglustaine, D. A. (2015). Assessment of the impact of oxidation processes on indoor air pollution using the new time-resolved INCA-Indoor model. *Atmospheric Environment*, *122*, 521–530. https://doi.org/10.1016/j.atmosenv.2015.10.025

Micolier, A., Berger, C., Rigault, B., & Mendez, M. (2020, November 1). *Identifying effective ventilation strategies to reduce COVID-19 infection risk indoors thanks to a multiroute transmission multi zonal model*. The 16th Conference of the International Society of Indoor Air Quality & Climate COEX, Seoul, Korea.

Morawska, L., Ayoko, G. A., Bae, G. N., Buonanno, G., Chao, C. Y. H., Clifford, S., Fu, S. C., Hänninen, O., He, C., Isaxon, C., Mazaheri, M., Salthammer, T., Waring, M. S., & Wierzbicka, A. (2017). Airborne particles in indoor environment of homes, schools, offices and aged care facilities: The main routes of exposure. *Environment International*, *108*, 75–83. https://doi.org/10.1016/j.envint.2017.07.025

Nazaroff, W. W., & Cass, G. R. (1986). Mathematical modeling of chemically reactive pollutants in indoor air. *Environmental Science & Technology*, *20*(9), 924–934. https://doi.org/10.1021/es00151a012

Nazaroff, W. W., & Cass, G. R. (1989). Mathematical modeling of indoor aerosol dynamics. *Environmental Science & Technology*, *23*(2), 157–166. https://doi.org/10.1021/es00179a003

Nørgaard, A. W., Kudal, J. D., Kofoed-Sørensen, V., Koponen, I. K., & Wolkoff, P. (2014). Ozone-initiated VOC and particle emissions from a cleaning agent and an air freshener: Risk assessment of acute airway effects. *Environment International*, *68*, 209–218. https://doi.org/10.1016/j.envint.2014.03.029

Otto, E., Fissan, H., Park, S. H., & Lee, K. W. (1999). The log-normal size distribution theory of brownian aerosol coagulation for the entire particle size range. *Journal of Aerosol Science*, *30*(1), 17–34. https://doi.org/10.1016/S0021-8502(98)00038-X

Pankow, J. F. (1994). An absorption model of the gas/aerosol partitioning involved in the formation of secondary organic aerosol. *Atmospheric Environment*, *28*(2), 189–193. https://doi.org/10.1016/1352-2310(94)90094-9

Pun, B. K., Seigneur, C., & Lohman, K. (2006). Modeling Secondary Organic Aerosol Formation via Multiphase Partitioning with Molecular Data. *Environmental Science & Technology*, *40*(15), 4722–4731. https://doi.org/10.1021/es0522736

Saathoff, H., Moehler, O., Schurath, U., Kamm, S., Dippel, B., & Mihelcic, D. (2003). The AIDA soot aerosol characterisation campaign 1999. *Journal of Aerosol Science*, *34*(10), 1277–1296. https://doi.org/10.1016/S0021-8502(03)00363-X

Sarwar, G., Corsi, R., Allen, D., & Weschler, C. (2003). The significance of secondary organic aerosol formation and growth in buildings: Experimental and computational evidence. *Atmospheric Environment*, *37*(9–10), 1365–1381. https://doi.org/10.1016/S1352-2310(02)01013-0

Sarwar, G., Corsi, R., Kimura, Y., Allen, D., & Weschler, C. J. (2002). Hydroxyl radicals in indoor environments. *Atmospheric Environment*, *36*(24), 3973–3988. https://doi.org/10.1016/S1352-2310(02)00278-9

Schoemaecker, C., Hanoune, B., Petitprez, D., Lebègue, P., Leclerc, N., Pingenot, X., Schneider, C., Verriele, M., Dusanter, S., Locoge, N., Le Calvé, S., Bernhardt, P., Mendez, M., Blond, N., Hauglustaine, D., Guo, F., Charpentier, I., Blondeau, P., & Abadie, M. (2015). *Projet MERMAID : Caractérisation détaillée de l'air intérieur des bâtiments énergétiquement performants par couplage entre Mesures Expérimentales Représentatives et Modélisation Air Intérieur Détaillée* (No. 1262C0023; Issue 1262C0023, p. 178). ADEME.

Shiraiwa, M., Ueda, K., Pozzer, A., Lammel, G., Kampf, C. J., Fushimi, A., Enami, S., Arangio, A. M., Fröhlich-Nowoisky, J., Fujitani, Y., Furuyama, A., Lakey, P. S. J., Lelieveld, J., Lucas, K., Morino, Y., Pöschl, U., Takahama, S., Takami, A., Tong, H., Sato, K. (2017). Aerosol Health Effects from Molecular to Global Scales. *Environmental Science & Technology*, *51*(23), 13545–13567. https://doi.org/10.1021/acs.est.7b04417

Siese, M., Becker, K. H., Brockmann, K. J., Geiger, H., Hofzumahaus, A., Holland, F., Mihelcic, D., & Wirtz, K. (2001). Direct Measurement of OH Radicals from Ozonolysis of Selected Alkenes: A EUPHORE Simulation Chamber Study. *Environmental Science & Technology*, *35*(23), 4660–4667. https://doi.org/10.1021/es010150p

Singer, B. C., Coleman, B. K., Destaillats, H., Hodgson, A. T., Lunden, M. M., Weschler, C. J., & Nazaroff, W. W. (2006). Indoor secondary pollutants from cleaning product and air freshener use in the presence of ozone. *Atmospheric Environment*, *40*(35), 6696–6710. https://doi.org/10.1016/j.atmosenv.2006.06.005

Tao, Y., & McMurry, P. H. (1989). Vapor pressures and surface free energies of C14-C18 monocarboxylic acids and C5 and C6 dicarboxylic acids. *Environmental Science & Technology*, *23*(12), 1519–1523. https://doi.org/10.1021/es00070a011

Thunis, P., Pederzoli, A., & Pernigotti, D. (2012). Performance criteria to evaluate air quality modeling applications. *Atmospheric Environment*, *59*, 476–482. https://doi.org/10.1016/j.atmosenv.2012.05.043

Tillmann, R., Hallquist, M., Jonsson, Å. M., Kiendler-Scharr, A., Saathoff, H., Iinuma, Y., & Mentel, Th. F. (2010). Influence of relative humidity and temperature on the production of pinonaldehyde and OH radicals from the ozonolysis of α-pinene. *Atmospheric Chemistry and Physics*, *10*(15), 7057–7072. https://doi.org/10.5194/acp-10-7057-2010

Tortajada-Genaro, L.-A., & Borrás, E. (2011). Temperature effect of tapered element oscillating microbalance (TEOM) system measuring semi-volatile organic particulate matter. *Journal of Environmental Monitoring*, *13*(4), 1017. https://doi.org/10.1039/c0em00451k

Tuovinen, S., Kontkanen, J., Cai, R., & Kulmala, M. (2021). Condensation sink of atmospheric vapors: The effect of vapor properties and the resulting uncertainties. *Environmental Science: Atmospheres*, *1*(7), 543–557. https://doi.org/10.1039/D1EA00032B

van Doremalen, N., Bushmaker, T., Morris, D. H., Holbrook, M. G., Gamble, A., Williamson, B. N., Tamin, A., Harcourt, J. L., Thornburg, N. J., Gerber, S. I., Lloyd-Smith, J. O., de Wit, E., & Munster, V. J. (2020). Aerosol and Surface Stability of SARS-CoV-2 as Compared with SARS-CoV-1. *New England Journal of Medicine*, *382*(16), 1564–1567. https://doi.org/10.1056/NEJMc2004973

Vartiainen, E., Kulmala, M., Ruuskanen, T. M., Taipale, R., Rinne, J., & Vehkamäki, H. (2006). Formation and growth of indoor air aerosol particles as a result of d-limonene oxidation. *Atmospheric Environment*, *40*(40), 7882–7892. https://doi.org/10.1016/j.atmosenv.2006.07.022

Wentzel, M., Gorzawski, H., Naumann, K.-H., Saathoff, H., & Weinbruch, S. (2003). Transmission electron microscopical and aerosol dynamical characterization of soot aerosols. *Journal of Aerosol Science*, *34*(10), 1347–1370. https://doi.org/10.1016/S0021-8502(03)00360-4

Winkler, P. M., Ortega, J., Karl, T., Cappellin, L., Friedli, H. R., Barsanti, K., McMurry, P. H., & Smith, J. N. (2012). Identification of the biogenic compounds responsible for size-dependent nanoparticle growth. *Geophysical Research Letters*, *39*(20), 2012GL053253. https://doi.org/10.1029/2012GL053253

Yasmeen, F., Vermeylen, R., Szmigielski, R., Iinuma, Y., Böge, O., Herrmann, H., Maenhaut, W., & Claeys, M. (2010). Terpenylic acid and related compounds: Precursors for dimers in secondary organic aerosol from the ozonolysis of α- and β-pinene. *Atmospheric Chemistry and Physics*, *10*(19), 9383–9392. https://doi.org/10.5194/acp-10-9383-2010